Chemical Engineering & Processing: Process Intensification 216 (2025) 110450

Contents lists available at ScienceDirect

Chemical Engineering and Processing - Process Intensification

journal homepage: www.elsevier.com/locate/cep

Crude palm stearin: A green and fast fractionation method to obtain a natural oil structuring agent

Diego Canizares [a,*], Tiago A.B.B. Cavalcante [b], Pedro A. Pessoa Filho [b], Maria A. Mauro [a]

[a] Institute of Biosciences, Humanities and Exact Sciences (IBILCE), Department of Food Engineering and Technology, São Paulo State University (UNESP), Rua Cristóvão Colombo, 2265, São José do Rio Preto 15054-000, Brazil

[b] Chemical Engineering Department, Engineering School, Universidade de São Paulo, Av. Prof. Luciano Gualberto, 380, Trav. 3, 05508-010 São Paulo, SP, Brazil

ARTICLE INFO

Keywords:
Crude palm oil
Crude palm stearin
Fractionation
Oleogel
Soybean oil structuration

ABSTRACT

This work investigated the effect of temperature control on crystallization and centrifugation of the crude palm oil aiming to fractionate it into crude palm stearin (CPS) and crude palm olein (CPO), and to explore the potential use of CPS as a structuring agent for soybean oil.Fractionation was carried out using a slightly modified oil-binding capacity method, where the temperatures of 10, 15, 20, and 25 °C were applied at crystallization and centrifugation. Purity of CPO was demonstrated through differential scanning calorimetry. Further, CPS fraction was evaluated as structuring agent for soybean oil carrying out differential scanning calorimetry, small-angle controlled stress dynamic rheology, polarized light microscopy, and X-ray diffraction analyses. A strong influence of temperature was observed on the CPS and CPO fractions yields. The 25 °C was considered the best temperature for crystallization and centrifugation. The CPS in soybean oil at 50 % (w/w) developed a solid-like behavior due to dispersion of needle-like crystal organized in cluster. Thermal and rheological behavior, and crystal-like morphology and crystallinity observed are similar to the frequently repported on organogels, indicating its potential as a natural and minimally processed ingredient or additive for food and pharmaceutical formulations.

1. Introduction

Palm crops have played a significant role in the economic development of Southeast Asia and West Africa over the past century, due to the increasing demand for palm fruit oil in industry and commerce [1]. Palm fruit is the source of crude palm oil and palm kernel oil. The FAO database indicates that crude palm oil is the most produced vegetable oil worldwide, surpassing soybean oil (SBO) production in 2006 (Fig. 1) [2].

Indonesia, Malaysia, and Thailand are the three major producers of crude palm oil [2]. Indonesia produced 256.6 million metric tonnes of crude palm oil in 2020, which accounts for 61.2 % of the world's production. The second largest producer was Malaysia, with an annual production of 91.4 million metric tonnes of crude palm oil in 2020, followed by Thailand, which produced 16.2 million metric tonnes of crude palm oil. These countries produced an average of 17.7 ± 0.5 metric tonnes of crude palm oil per hectare (ha) harvested per year. In turn, Nigeria, the fourth largest producer of crude palm oil, presents an average production yield of only 2.6 metric tonnes per hectare (ha) harvested per year [2]. Other relevant crude palm oil producers from Africa, such as Ivory Coast, Ghana, Guinea, and Congo, also presented a low average production yield of 5.6 ± 2 t of crude palm oil per hectare (ha) in 2020, which is closer to the 4 to 6 metric tonnes expected per hectare (ha) per year reported previously [3].

The drive behind this recent crude palm oil production growth is related to its unique fatty acid and triacylglyceride composition [4,5], allowing it to be applied in pharmaceutical formulations, as food ingredients, and as biodiesel [6]. The palm fruit pulp contains from 40 to 60 % of crude palm oil, which comprises approximately 50 % of saturated fatty acids and 50 % of unsaturated fatty acids [4,5,7]. Various authors observed that crude palm oil fatty acids are the lauric acid (C12:0), myristic acid (C14:0), palmitic acid (C16:0), palmitoleic acid (C16:1), stearic acid (C18:0), oleic acid (C18:1), linoleic acid (C18:2) and α-linolenic (C18:3), araquidic acid (C20:0), gadoleic acid (C20:1), bohenic acid (C22:0), lignoceric acid (C24:0) [5,7–9]. The same authors observed that palmitic acid (42.5 ± 1.8 %), oleic acid (40.8 ± 2.2 %) and linoleic acid (9.6 ± 0.8 %) constitute >90 % of the crude palm oil fatty acids [5,7–9]. The presence of high melting point compounds, such

* Corresponding author.
E-mail address: diego.canizares@unesp.br (D. Canizares).

https://doi.org/10.1016/j.cep.2025.110450
Received 29 April 2025; Received in revised form 19 June 2025; Accepted 14 July 2025
Available online 15 July 2025

as palmitic acid, and low melting point compounds, such as oleic and linoleic acids, results in the separation of two distinct fractions. The last step of palm oil refining process is the fractionation, where there is a separation of saturated fat acids from unsaturated fat acids, producing palm stearin and palm olein respectively [10,11].

Reddish color, strong flavor and its 1:1 saturated fat acids and unsaturated fat acids composition generate resistance from traditional industries for crude palm oil. There is a preference for more neutral lipids on their processes, protocols, methods, formulations and recipes. Wherefore, there is a tendency on the business-to-business market for demanding refined and modified palm oil, that can be used as frying medium or as ingredients for margarine, soft tube margarine, shortenings, ice creams, and blends [12–17]. Physical and chemical characteristics of crude palm oil are modified during refining, which process steps comprises degumming (physical refining process) or alkali neutralization (chemical refining process), bleaching, deodorization and fractionation [5,18]. Bleaching and deodorization are considered mandatory for producing refined palm oil, resulting in products with a wider range of applications in these previously mentioned traditional industries [12–15,17,19].

The refining process not only discourages the application of crude palm oil by minimally processed food industries but also may cause severe quality degradation. Kim-Tiu *et al.* [20] observed that crude palm oil is naturally trans fatty acid free, but after refining the derivatives may present fractions of trans fatty acids. Health agencies throughout the world, such as the World Health Organization (WHO), the United States Department of Agriculture (USDA), the European Commission (European Union), Health Canada (Canada), and ANVISA (Brazil), have intensified warnings about trans-fatty acid consumption because of its high potential to increase low-density lipoprotein, LDL, and reduce high-density lipoprotein, HDL [21–23]. Easy access to information and growing concern about quality of life have changed people's consumption profiles, intensifying the demand for healthier products [24–26]. Consequently, greener, more natural, and less processed food products have received increasing attention [24–26].

In many countries, unrefined crude palm oil is used in traditional dishes. In Brazil, unrefined crude palm oil is popular in the northeast region, where it is called *Azeite de Dendê* and is incorporated into many recipes, for example: *acarajé, bobó, caruru, moqueca*, and *vatapá*. Due to temperature fluctuation, unrefined crude palm oil may be found or as a bi-phase or as a solid-like product at market counters. This empiric observation implies that temperature and density could be applied to isolate saturated fat acids from unsaturated fat acids, and that the saturated fat acids from crude palm oil could function as a structuring agent. Henceforth, to avoid misunderstandings with the refined fractions from palm oil, palm stearin and palm olein, the unrefined fractions will be referred to as crude palm stearin (CPS) and crude palm olein (CPO).

Palm stearin is usually obtained by dry fractionation of bleached and deodorized palm oil throughout crystallization of palm stearin fraction at a controlled temperature followed by separation in filter presses or vacuum filters [9,11,27–30]. Other authors have proposed solvent fractionation methods, which is out of the scope of this work [31]. At this point, two pertinent questions may be raised. The first one concerns to the rationale behind the omission in evaluating centrifugation as an industrial method for fractionating crude palm oil, given its accelerated decantation process and its potential for operating under controlled temperature. In recent study, the application of centrifugation in virgin coconut oil production demonstrated significant potential, yielding promising outcomes [32]. The second question lies in the missing information about possible application CPS to structure other oils. Margarine industry, for instance, could take great advantage of a natural reddish structuring agent, since commercial margarines are enriched with structuring agents (fully hydrogenated fats and modified palm and palm kernel oils) and food coloring (curcuma, carotenes, yellow color n° 5 and yellow color n° 6) to reach the expected yellowish solid-like product.

A continuous centrifuge can handle processing capacities of up to 300 m^3/h [33]. A recent research project successfully reduced the power consumption of large-volume rate centrifuges to <0.5 kWh/m^3, achieving a consumption of 0.25 kWh/m^3 in certain conditions [34]. In comparison, a commercial rotary vacuum drum filter with 25 m^2 can filter up to 112.5 m^3/h, achieving a theoretical consumption of 0.4 kWh/m^3 [35]. Nevertheless, the power requirements for the vacuum and filtrate pumps are not included in this calculation. Filter presses are cost-effective alternatives to centrifuges and vacuum filtration because they are affordable, easy to operate, and energy-efficient [36,37]. However, the filtration of crude palm oil using filter presses is hindered by two primary issues: the filtration rate is approximately 15 L/m^2h, which is considered low, and due to the high concentration of solids there is a rapid cake formation, which reduces the filtration rate and demands more frequent cake discharging procedures [38–40]. Filter pressing, vacuum filters and centrifugation are all solvent free fractionation methods. This is beneficial from a sustainability perspective, because even a green solvent such as ethanol would require processing, transportation, and waste disposal control.

Thus, the two primary objectives of this study were to propose an alternative solvent-free fractionation process for crude palm oil, based on temperature-controlled crystallization and centrifugation, and to investigate the potential of CPS as structuring agent of soybean oil (SBO).

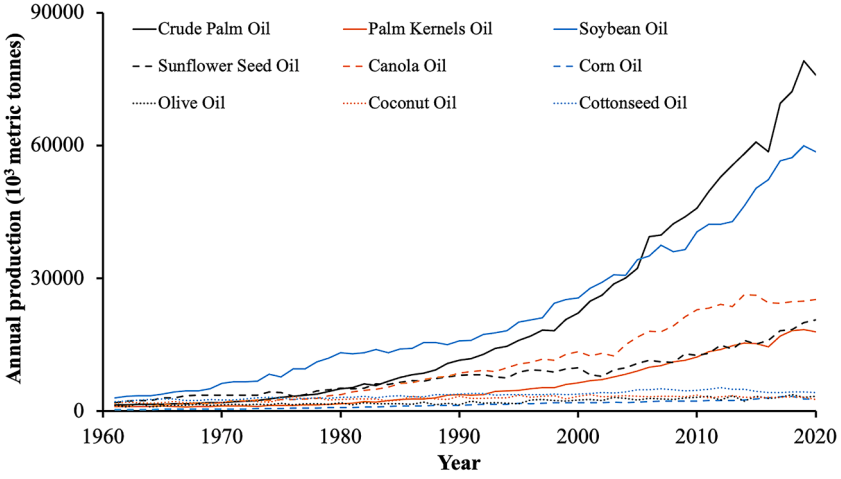

Fig. 1. World's annual production of the most important vegetable oils from 1960 to 2020 [2].

2. Materials and methods

2.1. Best condition for crude palm oil fractionation

The fractionation was carried out using a centrifugation method slightly modified from the oil-binding capacity determination reported by Canizares *et al.* [41,42]. Commercial crude palm oil (Opalma®, Óleos de Palma S/A) was transferred to a glass beaker (250 mL) and heated at 90 °C for 30 min using a hot plate with magnetic stirring (Model 114, Nova Ética®, Brazil). Samples of 1 g of crude palm oil were placed in previously weighted Eppendorf tubes (1.5 mL). These tubes were stored at 10, 15, 20, and 25 °C in a controlled temperature chamber (MA830/A, Marconi®, Brazil) for 24 h. The samples were then centrifuged for 15 min with a relative centrifugal force of 12,000 × *g* (Z326K, Hermle®, Germany) at constant temperatures of 10, 15, 20, and 25 °C. After centrifugation, the supernatant oil phase was drained, and the remaining sample was weighted to determine the oil-binding capacity. Analyses were carried out in triplicate.

2.2. Fractionation of CPS

The optimal temperature conditions for fractionation were determined previously and applied with minor modifications to obtain the CPS fraction. Commercial crude palm oil was heated at 90 °C in a glass beaker (500 mL) for 30 min on a hot plate with magnetic stirring (Model 114, Nova Ética®, Brazil). Samples of approximately 40 mL of crude palm oil were then transferred to Falcon tubes (50 mL). Samples were kept in a controlled temperature chamber (MA830/A, Marconi®, Brazil) at the best storage temperature for 24 h and then centrifuged for 15 min at a relative centrifugal force of 12,000 × *g* (Z326K, Hermle®, Germany) at the optimal temperature. Supernatant oil (CPO) and sedimented fat (CPS) were separated, placed in sealed plastic containers, and stored at 4 °C until required.

2.3. Critical concentration

The critical concentration is the minimal amount of solute needed to structure a solvent to form an organogel [41–43]. The concentration of CPS needed to structure the commercial SBO (Liza®, Cargill S/A) was determined following the methodology previously presented by Canizares *et al.* [41,42]. Dispersions of CPS in SBO were prepared in test tubes with stearin mass fractions ranging from 2 % to 72 %. These dispersions were heated at 90 °C for 60 min using a dry block (MA4004, Marconi®, Brazil) to ensure complete melting and solubilization of the CPS crystals. The samples were then kept at 25 °C in a controlled temperature chamber (MA830/A, Marconi®, Brazil) for 24 h. The critical concentration of CPS in SBO was determined visually by turning the test tubes to check the flow capability [41]. Analyses were carried out in triplicate.

2.4. Differential scanning calorimetry

Samples (8–15 mg) of crude palm oil, CPS, CPO, SBO, and dispersion of CPS in SBO at the critical concentration were placed in 20 μL aluminum pans (Model 02,190,062, PerkinElmer). The analyses were carried out in a differential scanning calorimeter Model 3+ with FRS 6+ sensor (Mettler Toledo, Switzerland) using the following temperature protocol: heating from 25 °C to 90 °C at a rate of 20 °C.min^{-1}, isothermal at 90 °C for 30 min, cooling to −30 °C at a rate of 5 °C.min^{-1}, followed by isothermal at −30 °C for 30 min, and heating from −30 °C to 90 °C at a rate of 5 °C.min^{-1} [41,42]. The onset crystallization temperature and the endset melting temperature were determined from the cooling and last heating steps, respectively (Fig. 2), using STARe Evaluation software (v.17.00, Mettler Toledo, Switzerland). All the analyses were performed in duplicate for each treatment.

2.5. Small angle controlled stress dynamic rheology

The storage modulus (G') and yield stress of the crude palm oil and dispersion of CPS in SBO at the critical concentration were determined via a stress sweep using a TA Instruments AR2000 Controlled Stress Rheometer (New Castle, DE, USA) equipped with crosshatched parallel plates (40 mm) and a Peltier system (± 0.1 °C) acting under the lower plate. The solutions were preheated at 90 °C for 30 min and transferred to the rheometer lower plate. The gap between plates was adjusted to 0.9 ± 0.1 mm. Before analysis, the solutions underwent a temperature protocol of three isothermal steps of 30 min each [41–44]. The protocol began with a step at 90 °C, followed by a step at 0 °C, and a final step at 25 °C. Analyses were carried out at 25 °C to determine the G' and yield stress of the samples at a constant frequency of 1 Hz. The yield stress was considered to be the stress at which G' exited the linear viscoelastic region. The results were obtained in duplicate.

2.6. Crystal-like structure morphology

The crystal-like structure morphology analysis was performed following the procedure presented by Canizares *et al.* [42] with minor alterations. The morphology of crystal-like structures presented in crude palm oil and in the dispersion of CPS in SBO at the critical concentration were evaluated using a polarized light microscope BX-51 (Olympus,

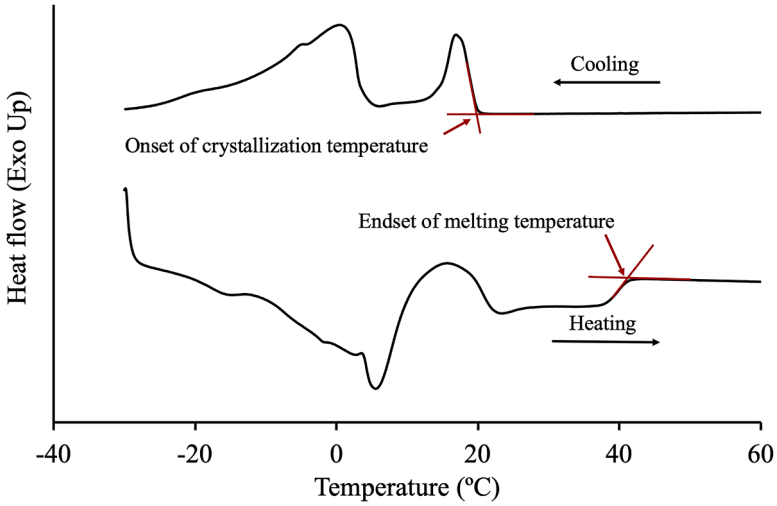

Fig. 2. Example of DSC thermogram illustrating the procedure to determine the onset of crystallization temperature and the endset of melting temperature.

Tokyo, Japan) with a camera DP-21 (Olympus). The samples were preheated at 90 °C for 30 min, and one drop was placed on microscope slides and kept at 25 °C in a controlled temperature chamber (MA830/A, Marconi®, Brazil) for 24 h. The morphology analysis of crystal-like structures was performed in triplicate, and pictures were taken at four different positions on each slide at 10X and 40X magnification. Analyses were carried out in triplicate.

2.7. Porosity

Porosity was determined following the methodology described by Canizares *et al.* [41,42] using ImageJ® (1.52a, National Institute of Health, Bethesda, Maryland, USA). The porosity was determined for all images obtained in the morphology analysis of crystal-like structures at 10X magnification.

2.8. Crystalline structure and relative crystallinity

X-ray diffraction (XRD) of crude palm oil and the dispersion of CPS in SBO at the critical concentration were conducted on a Rigaku MiniFlex 600 (Rigaku, USA). Sample holders with wells (0.5 mm depth) were loaded with samples previously melted at 90 °C for 30 min and, then, kept at room temperature for 24 h until analysis. Angular scans (2θ) were performed from 4° to 40° at 1.2 min−1 using a Cu (λ = 0.154 nm) tube at 30 kV and 10 mA as the X-ray source. Bragg's law was applied to determine the d-spacing between lattices [41–43]. All the measurements were performed at 25 °C.

Relative crystallinity can be estimated from the X-ray diffraction graphs (Fig. 3, gray line) by the ratio of the total area of the crystalline phase to the total area of both the crystalline and amorphous phases [45]. The relative areas of the peaks were determined using a methodology adapted from the study by Polizzi *et al.* [46]. The background scattering was obtained using the geometric moving average, considering a period of 41 points, from 20 points before to 20 points after the desired point (Fig. 3, black line). Then, the total area and background scattering area under the curves were determined, allowing the calculation of the relative crystallinity [45,46].

2.9. Statistical analysis

Analyses were performed at least in duplicate, and the results were analyzed using ANOVA at a 5 % significance level. The Tukey–Kramer's test was applied to locate significant differences between samples at the 5 % significance level. All the analyses were performed using SAS (v. 9.4, SAS Institute Inc., Cary, NC, USA) [47].

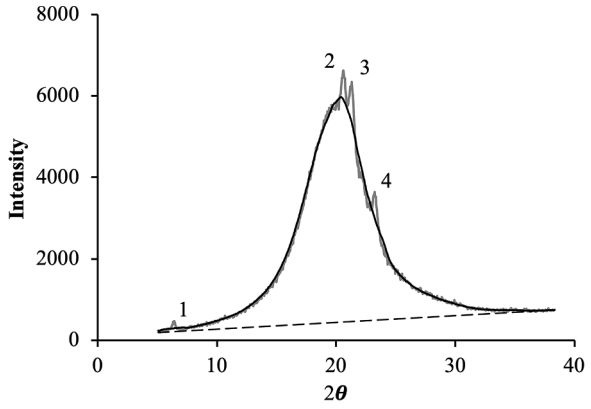

Fig. 3. Illustration of an expected X-ray diffraction pattern (Fig. 3, gray line) with 4 peaks indicating the presence of crystals, a curve without peaks (Fig. 3, black line) used as base to determine the area of the peaks by difference, and a baseline (black dashed line).

3. Results

3.1. Best condition for CPS fractionation

The results of the oil-biding capacity analysis of crude palm oil are presented in Table 1. The objective of this analysis was to determine the amount of lipids that could be attached to crystalline structures (fat crystals) under certain temperature conditions [41,42,48]. Fat crystals and attached lipids formed a solid deposit at the bottom of the Eppendorf tubes after centrifugation. This solid has a paste-like appearance, whereas the oil that is not bound to the crystals is present as a supernatant. These fractions are referred to as CPS and CPO, respectively. The mechanism explaining the oil-binding capacity of the crystals is still not fully understood. Some authors have considered that oil may be stuck between the crystalline structures [41,42]. The morphology, concentration, and density of the crystals are frequently related to their oil-binding capacity [41–43].

The results presented in Table 1 show the strong influence of temperature on the oil-biding capacity of crude palm oil. Samples stored at 10 and 15 °C and centrifuged at 10 °C presented 100 % oil-binding capacity, precluding the separation of CPS and CPO. The oil-binding capacity decreased significantly with an increase in the storage and centrifugation temperatures (Table 1), allowing the separation of CPS and CPO. The best storage and centrifugation temperature for fractionating crude palm oil was determined to be 25 °C. There are two main reasons for this finding. First, this temperature is close to the possible plant operating conditions in tropical countries, where crude palm oil is usually processed. Second, this temperature yields a fraction of palm stearin in palm oil close to 50 %, close to the value usually reported in the literature [5,7].

The results of the applied centrifugation method can be compared to those of other previously reported fractionation methods. The vacuum filter fractionation of crude palm oil carried out by Kumar and Krishna [28] presented a yield of 77 % for CPO and 23 % for CPS. This discrepancy can be ascribed to the fact that high melting point compounds may have passed through the filter, as the oil is expected to contain about 43 % palmitic acid [5,8,7], which roughly corresponds to the minimum value of the stearin fraction. Another hypothesis is that the sample analyzed by the authors had a lower concentration of CPS. Zaliha et al. [10] evaluated the effect of the crystallization temperature on the chemical composition of CPO and CPS fractionated through vacuum filtration. They observed that reducing the crystallization temperature from 18 °C to 9 °C resulted in a lower concentration of saturated fatty acids in CPO olein. Unfortunately, the authors did not report the yield of each fraction after separation.

To evaluate the purity of the CPS and CPO obtained from the chosen fractionation method at the optimal temperature conditions, DSC analysis of crude palm oil, CPS, and CPO was carried out (Fig. 4). As described in Section 2.4, the samples were initially heated to 90 °C to

Table 1
Oil-binding capacity analysis optimization of CPO following storage temperature in a controlled temperature chamber (10 °C, 15 °C, 20 °C, and 25 °C) and centrifugation temperature (10 °C, 15 °C, 20 °C, and 25 °C) at 12,000 × *g* force.

		Centrifuge temperature (°C)			
		10	15	20	25
Chamber temperature (°C)	10	100.07 ± 0.22^{a}	100.07 ± 0.22^{a}	98.69 ± 0.77^{b}	68.54 ± 1.55^{d}
	15	100.01 ± 0.06^{a}	96.12 ± 0.85^{b}	84.58 ± 1.99^{c}	58.99 ± 1.72^{e}
	20	68.16 ± 1.33^{d}	69.09 ± 1.32^{d}	60.59 ± 1.47^{e}	58.19 ± 1.09^{e}
	25	46.02 ± 1.20^{f}	48.5 ± 0.72^{f}	45.52 ± 0.74^{f}	46.19 ± 1.03^{f}

Means followed by different lowercase letters are significantly different ($p < 0.05$) according to Tukey's test.

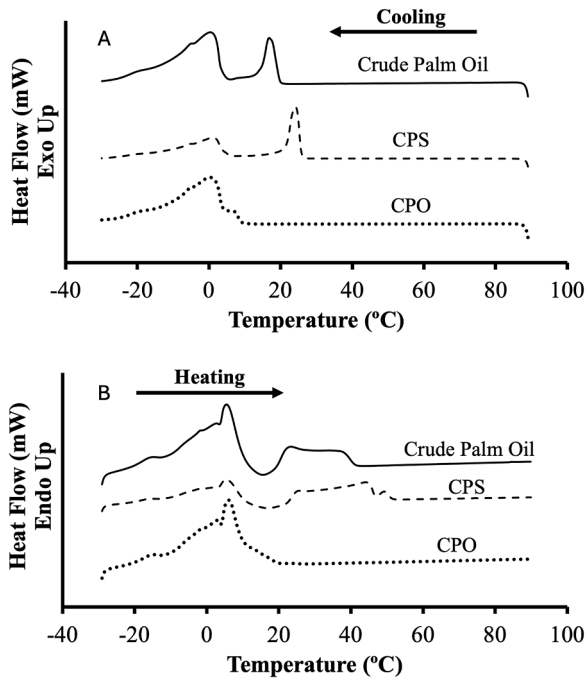

Fig. 4. Crystallization (A) and melting (B) behavior of Crude Palm Oil, CPS, and CPO determined through DSC analysis.

ensure complete fat crystal melting. The samples were then cooled to −30 °C (Fig. 4A) to evaluate the crystallization, followed by heating to 90 °C to evaluate the melting behavior (Fig. 4B).

The most relevant information in Fig. 4 is the difference between the thermal behavior of crude palm oil and CPO. For CPO, only one peak was observed at temperatures lower than 20 °C during the cooling (Fig. 4A) and heating (Fig. 4B) curves. This indicates that the fraction of lipids with a high melting point in crude palm oil is not present in CPO. This behavior is similar to that observed by Zaliha *et al.* [10] from thermograms of olein and stearin fractions.

Fig. 4 also shows that the onset crystallization temperature (Fig. 4A) and endset melting temperature (Fig. 4B) of CPS are higher than those of crude palm oil. This indicates that the concentration of high-melting-point compounds in CPS is higher than in crude palm oil. Similar thermal behavior has been frequently reported for different wax concentrations in vegetable oil organogels [41,42]. Briefly, the absence of a high melting point peak at the CPO and the shift of the high melting point peak at the CPS can be considered as validations of the fractionation method.

The average values of the onset crystallization temperature for crude palm oil (19.7 ± 0.3 °C), CPS (27.1 ± 1.9 °C), and CPO (10 ± 1.4 °C) were significantly different according to Tukey's test ($p < 0.05$). Similar observation was made for the average values of the endset melting temperature of crude palm oil (41.1 ± 0.1 °C), CPS (51.3 ± 0.3 °C), and CPO (19.8 ± 0.7 °C), according to Tukey's test ($p < 0.05$). Therefore, CPS may be considered to have the highest concentration of high-melting-point compounds, while CPO has the lowest temperatures of crystallization and melting and does not present a peak at high temperatures.

3.2. Critical concentration

The visual appearance of the CPS dispersed in SBO at concentrations between 2 and 72 % (w/w) is shown in Fig. 5. No structuration was observed at CPS concentrations lower than 48 % (w/w) (Fig. 5A, 5B, 5C, and 5D). Figure (5E) shows that samples with concentrations ranging from 52 to 72 % (w/w) presented structuration at 25 °C. To improve the precision of the analysis, a second set of experiments was carried out for samples with 49, 50, and 51 % (w/w) of CPS in SBO (Fig. 5F). The analysis of Fig. 5F shows that the critical concentration of CPS in SBO was 50 % (w/w). The dispersion of CPS in SBO at a critical concentration was chosen for further analysis and is referred to as CPS in SBO.

3.3. Small-angle controlled stress dynamic rheology

The apparent structuration of the samples was assessed using small-angle controlled stress dynamic rheology (Fig. 6). For comparison purposes, rheological analysis was carried out for samples of crude palm oil and CPS in SBO at the critical concentration.

The storage modulus presented an average value of 3.0×10^5 Pa for crude palm oil and 4.8×10^4 Pa for CPS in SBO at the critical concentration (50 %, w/w). These values were at the same order of magnitude as those reported by Blake et al. [43] for canola oil organogels at critical concentrations prepared from rice bran wax (1 %), sunflower wax (1 %), candelilla wax (2 %), and carnauba wax (4 %).

The linear viscous-elastic regions of the storage modulus (G') are higher than the loss modulus (G'') for both samples, which demonstrates the crude palm oil and the SBO structuration. Furthermore, the higher G' value and the absence of yield stress for crude palm oil within the analyzed stress range indicate that it has more stable solid characteristics compared to CPS in SBO at the critical concentration at 25 °C. A possible explanation to this better solid behavior of crude palm oil may be linked to the crystal-crystal and crystal-liquid interactions responsible for the sample structuration, where CPS crystals present a higher number or a more favorable interaction with CPO than with SBO [41, 42].

3.4. Differential scanning calorimetry

The thermal behavior during the cooling and heating of SBO, CPS, and CPS in SBO at the critical concentration (50 % w/w) is presented in Fig. 7. CPS in SBO presented a lower onset of crystallization and endset of melting temperatures (Fig. 7A and 7B, respectively) than CPS. This reduction is related to CPS solubilization in SBO, which lowers the thermodynamic activity of CPS (here understood as a single pseudo-component) and consequently lowers the melting temperature. The CPS in SBO presented 21 ± 0.4 °C as the onset of crystallization temperature, which is statistically equivalent to the onset crystallization temperature observed for crude palm oil (Fig. 4). The SBO onset of crystallization temperature is −7.5 ± 0.5 °C (Fig. 7), significantly lower than that of all the other samples analyzed in this work (Figs. 4 and 7). Since it is possible to assume that crude palm oil is a dispersion containing approximately 50 % (w/w) of CPS in CPO (Table 1), this finding indicates that CPO and SBO may have similar CPS saturation.

At Fig. 7B, the average melting point of CPS (51.3 ± 0.3 °C) and CPS in SBO at the critical concentration (48.5 ± 0.4 °C) did not present significant difference according to Tukey's test ($p < 0.05$). Furthermore, the melting points of CPS and CPS in SBO at the critical concentration are close to the melting point of roll-in shortening, which is widely used in puff and Danish pastry products which require lamination [49,50]. The onset crystallization temperatures of SBO (−7.6 ± 0.3 °C) was significantly lower than those of CPS (27.1 ± 1.9 °C) and CPS in SBO at the critical concentration (21 ± 0.2 °C) according to Tukey's test ($p <$ 0.05).

3.5. Crystal morphology and relative crystallinity

To observe the crystal-like structural morphology, crude palm oil and CPS in SBO were evaluated using optical microscopy with polarized light (Fig. 8). The crude palm micrographs show spherical clusters of needle-like structures of uneven sizes (Fig. 8A and 8B). Crystal-like structures of CPS in SBO at critical concentration also present a needle-like morphology organized in clusters (Fig. 8C and 8D), but they are smaller than those observed in crude palm oil (Fig. 8A and 8B). The

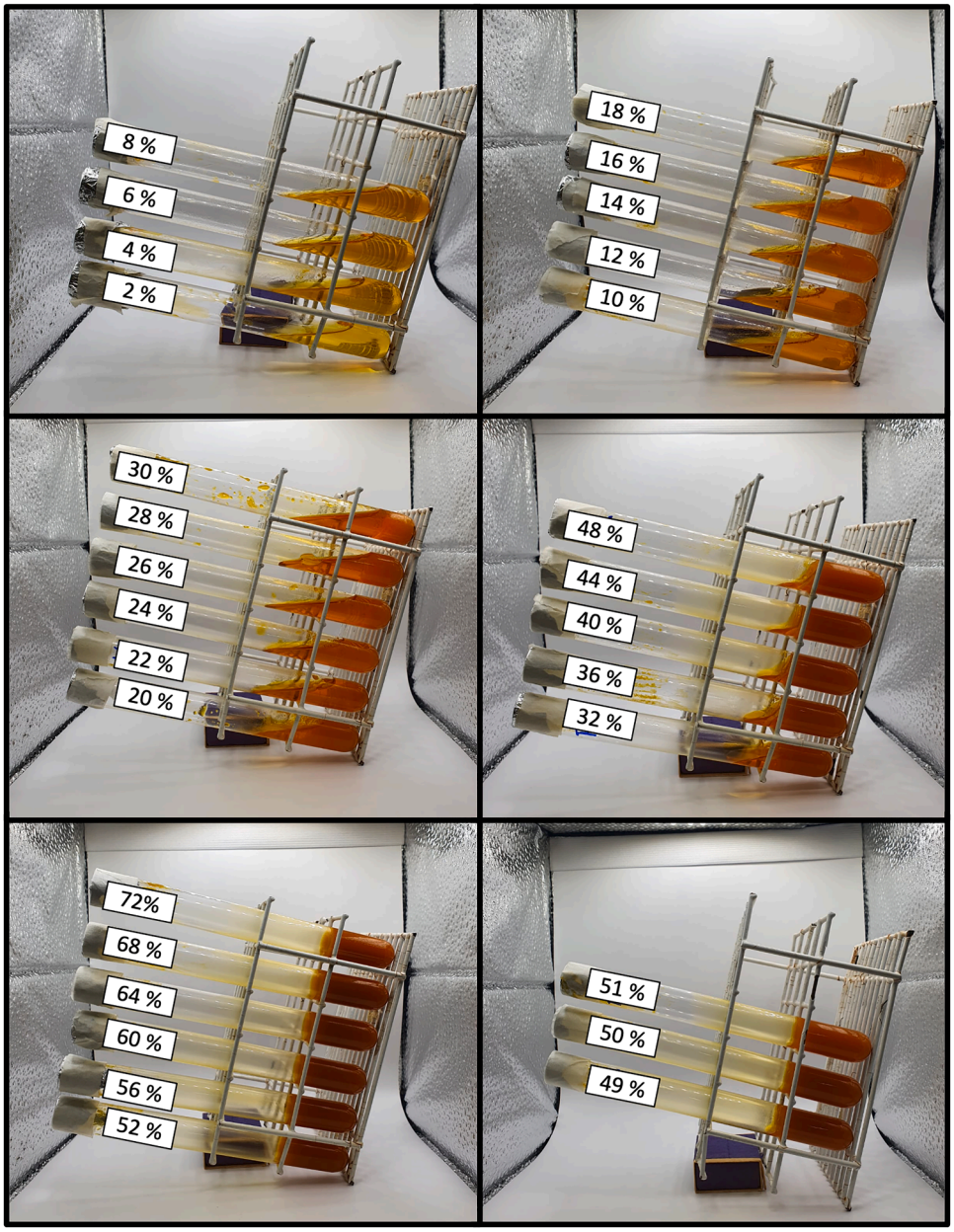

Fig. 5. Samples of CPS dispersed in SBO at different concentrations for critical concentration determination.

clusters formed in the crude palm oil solution are not organized, resembling the formation of a 3D crystal network. Although crystal-like structures organized in clusters are considered less effective than isolated needle-like crystals in preventing oil migration, cluster structures tend to be more palatable [41,42,48]. Authors have emphasized the influence of crystal size on mouthfeel during sensory analysis, noting that 50 μm is the threshold for crystal perception in the mouth [41,42,47].

The porosities of crude palm oil and CPS in SBO were 46.1 ± 3.9 % and 36.8 ± 9.2 %, respectively. The average porosities obtained from micrographs of crude palm and CPS in SBO were significantly different ($p < 0.05$) according to Tukey's test. This means that crude palm oil presents significantly higher inter-crystalline spaces than CPS in SBO. It is interesting to observe how the rheological characteristics analyzed for crude palm oil and CPS in SBO are not directly related to the porosity, in concordance with previous works for oleogel [41–43].

3.6. Crystal structure

The X-ray diffraction patterns of crude palm oil and CPS in SBO at the critical concentration are shown in Fig. 9. Both patterns are characteristic of crystalline structures. Peaks indicating interlaminar latices distance of 14 Å, 4.32 Å, 4.20 Å, and 3.85 Å are observed for crude palm oil. For the system at the critical concentration, the interlaminar lattice distances observed were 4.55 Å, 4.43 Å, 4.25 Å, 4.14 Å, and 3.86 Å, which are frequently associated with needle-like crystals [41,42]. According to various authors [41,51–53], a slight shift in the interlaminar lattice distance may be observed from one sample to another. Two peaks are often related to needle-like crystals, the first one is observed at the range from 4.07 Å to 4.21 Å, and the second one is observed from 3.66 Å to 3.82 Å [41–43,51–53]. This shift is probably due to the interference of the medium, because the X-ray diffraction technique and Bragg's law were developed for powders.

The size of the peaks in Fig. 9 indicates the relative crystallinity of the solution [45], which usually does not correlate with the size and

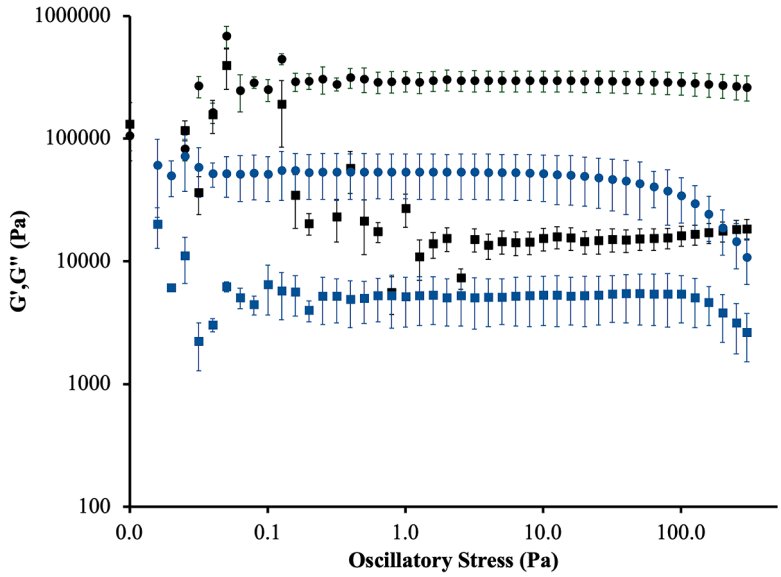

Fig. 6. Means and standard deviation of storage modulus (G', circles) and loss modulus (G'', squares) of Crude Palm Oil (black color) and of CPS in SBO at critical concentration (blue color) during small-angle controlled stress dynamic rheology analysis.

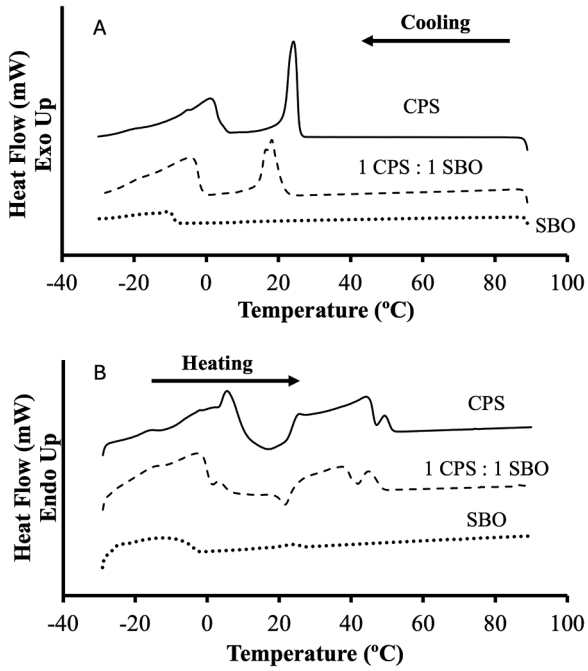

Fig. 7. Crystallization (A) and melting (B) behavior of CPS, CPS in SBO at critical concentration and SBO determined through DSC analysis.

distribution of the crystals seen in the micrographs (Fig. 8). This fact may be misleading because micrographs suggest the presence of a fraction of crystal-like structures larger than the effective quantity of crystalline structures present in the sample. The relative crystallinities of crude palm oil and CPS in SBO estimated from the X-ray diffraction pattern graphics were 2.1 ± 0.9 % and 1.25 ± 0.12 %, respectively. Both X-ray diffraction patterns and calculated crystallinity values correspond to the solid fat content determined for oleogels at critical concentration [41–43,51–53]. Furthermore, the values for crystallinity are considerably lower than the area occupied by the crystal-like structures in the micrographs (Fig. 8). Similar behavior was observed by Blake *et al.* [43] and Canizares *et al.* [42]. These authors observed significant discrepancies between the crystallinity directly determined by NMR and the area occupied by crystal-like structures in micrographs. This suggests that the structures observed in Fig. 8 may also comprise amorphous patches that are scarcely distinguishable from the crystalline structures at these magnifications. Another factor that may account for this difference is the light refringence in amorphous phases. For instance, Hartel [48] stated that the vicinity of the crystalline structure in crystal-saturated solutions comprises a supersaturated layer where equilibrium mass exchange between solid and liquid occurs. This supersaturated solution layer is stagnated because of the boundary effect (no-slip condition) related to the corresponding transport phenomenon [54]. This stagnation and supersaturation may give this layer the characteristics of an amorphous phase and, consequently, refringence properties like those of the amorphous polymers studied by Inoue [55].

4. Conclusion

The experimental procedure that comprises a crystallization period of 24 h at 25 °C followed by centrifugation at the same temperature constitutes a feasible alternative dry method to a fast fractionation of crude palm oil into CPO and CPS. Although the procedure was investigated only at the laboratory scale, it constitutes a promising alternative to be considered for industrial-scale fractionation processes, as it comprises few unit operations with low environmental impact.

Analyses in DSC demonstrated that high-melting-point molecules from crude palm oil were not present in the CPO fraction. Furthermore, the increase of the onset of crystallization temperature and the endset of melting temperature of CPS, relative to crude palm oil, indicates a higher concentration of high-melting-point molecules in the CPS fraction. These findings validate the fractionation. The CPS fraction promoted the structuration of SBO, which indicates its high potential as a minimally processed ingredient in food products. The low crystallinity is advantageous for food products mouthfeel.

To conclude, a wide range of potential future research opportunities has emerged from these results. For instance, the following questions could be considered for study: the feasibility of scaling-up the fractionation process by using industrial centrifuges; the synergy between CPS and fats or waxes on the structuration of vegetable oils; the quality of biodiesel produced from CPO; the shelf life stability of the CPO in comparison to crude palm oil; the sensory acceptance of CPS added food products; among others.

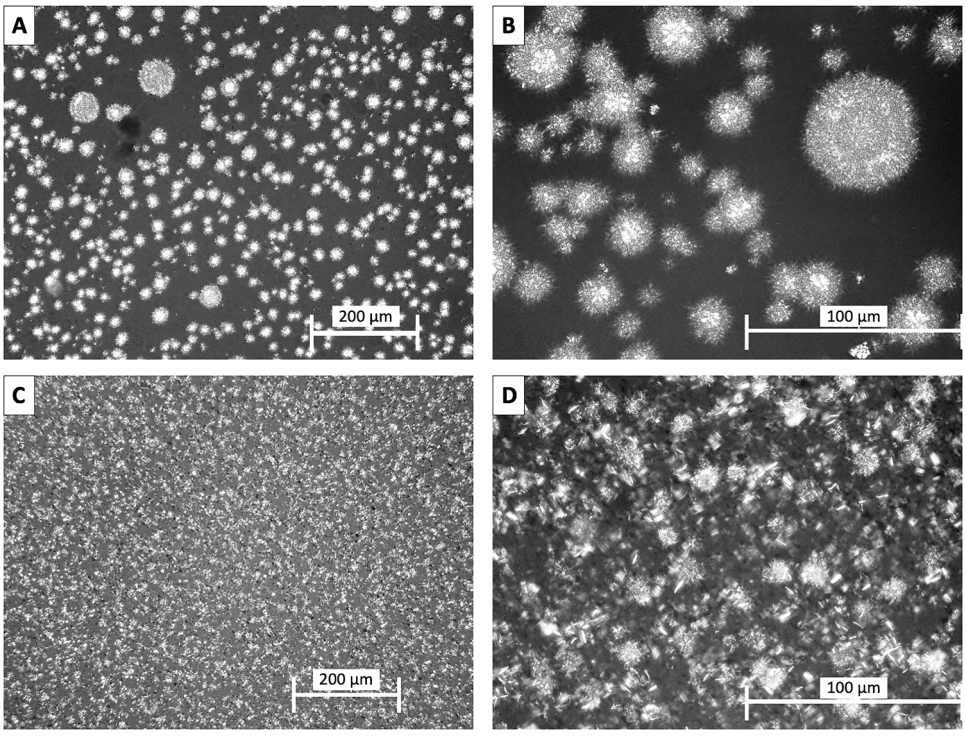

Fig. 8. Micrographs showing crystalline structures on Crude Palm Oil (A, B) and on CPS in SBO at the critical concentration (C, D). Images (A) and (C) were obtained with 10X magnification, and images (B) and (D) were obtained with 40X magnification.

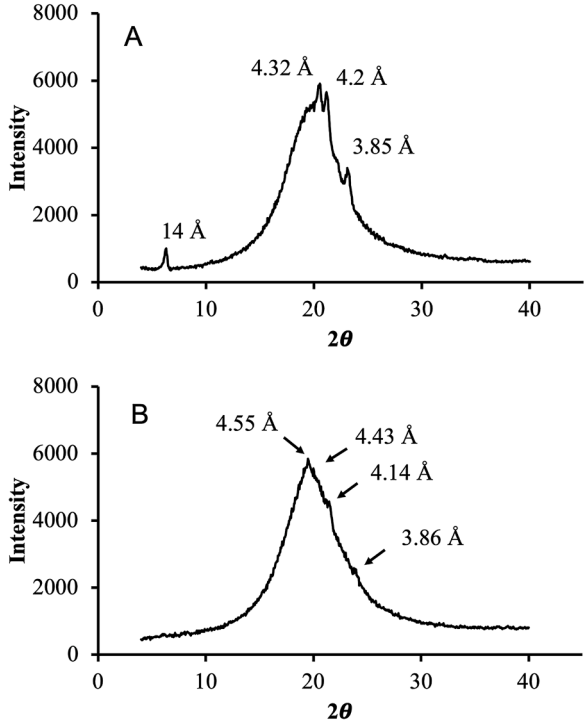

Fig. 9. X-ray diffraction patterns of Crude Palm Oil (A) and CPS in SBO at critical concentration (B).

CRediT authorship contribution statement

Diego Canizares: Writing – review & editing, Writing – original draft, Visualization, Validation, Resources, Methodology, Investigation, Funding acquisition, Formal analysis, Data curation, Conceptualization. **Tiago A.B.B. Cavalcante:** Methodology, Investigation, Formal analysis. **Pedro A. Pessoa Filho:** Writing – review & editing, Supervision, Formal analysis, Data curation. **Maria A. Mauro:** Writing – review & editing, Validation, Supervision, Resources, Project administration, Funding acquisition.

Declaration of competing interest

The authors declare the following financial interests/personal relationships which may be considered as potential competing interests:

Acknowledgements

The authors would like to thank the Brazilian agencies Fundação de Amparo à Pesquisa do Estado de São Paulo (FAPESP), processes 2020/02734-5 (scholarship to D.C.), 2020/05254-4 (financial support to M.A.M.), and 2022/06033-7 (scholarship to T.A.B.B.C.), and Conselho Nacional de Desenvolvimento Científico e Tecnológico (CNPq), process 308882/2023-7 (P.A.P.F.). The authors would also like to thank all the professionals from the Laboratory of Cereals (IBILCE/UNESP, São José do Rio Preto) for making available the X-ray diffractometer, from the Physical Properties Laboratory (IBILCE-UNESP, São José do Rio Preto) for allowing us to use the rheometer, from the Multiuser Center for Microscopy and Microanalysis facilities (IBILCE-UNESP, São José do Rio Preto) for sharing with us the light microscope, and from the Analysis and Thermal Studies and of Equilibrium in Food (POLI-USP, São Paulo) for the assistance and cooperation with the DSC thermal analyses.

Data availability

Data will be made available on request.

References

[1] M.F. Hasan, I. Fadhil, M.M. Fahmid, T. Ahmad, Impact of the European Union regulations on Indonesian oil palm smallholder farmers, Int. J. Oil Palm 5 (1) (2022), https://doi.org/10.35876/ijop.v5i1.69.

[2] FAO. [FAOSTAT]. License: CC BY-NC-SA 3.0 IGO. Accessed: JulyExtracted from: https://www.fao.org/faostat/en/#data/QI. Data of Access: 15/07/2023.

[3] N.N. Godswill, N.E.G. Frank, A.N. Walter, M.Y.J. Edson, T.M. Kingsley, V. Arondel, B.J. Martin, Y. Emmanuel, Oil palm, in SK Gupta. Breeding Oilseed Crops For Sustainable Production, 1st Ed., Elsevier, 2016, pp. 217–273, https://doi.org/10.1016/B978-0-12-801309-0.00010-0.

[4] K.G. Berger, Trans-free fats with the products of the oil palm - a selective review, Czech J. Food Sci. 25 (4) (2007) 174–181, https://doi.org/10.17221/688-CJFS.

[5] I.N. Aini, M.S. Miskandar, Utilization of palm oil and palm products in shortenings and margarines, Eur. J. Lipid. Sci. Technol. 109 (4) (2007) 422–432, https://doi.org/10.1002/ejlt.200600232.

[6] A. Kaewchada, N. Akkarawatkhoosith, D. Bunpim, T. Bangjang, C. Ngamcharussrivichai, A. Jaree, Production of bio-hydrogenated diesel from palm oil using Rh/HZSM-5 in a continuous mini fixed-bed reactor, Chem. Eng. Process. 168 (2021), https://doi.org/10.1016/j.cep.2021.108586.

[7] M.H.M. Buscato, B.G. Zaia, K.R.R.D. Godoi, A.P.B. Ribeiro, T.G. Kieckbusch, Modification of palm oil crystallization by phytosterol addition as a tool for structuring a low saturated lipid blend, Braz. J. Chem. Eng. 35 (1) (2018) 169–180, https://doi.org/10.1590/0104-6632.20180351s20160351.

[8] D.T. Almeida, I.L. Nunes, P.L. Conde, R.P.S. Rosa, W.F. Rogério, E.R Machado, A quality assessment of crude palm oil marketed in Bahia, Brazil, Grasas Aceites 64 (4) (2013) 387–394, https://doi.org/10.3989/gya.118412.

[9] D.J. Murphy, K. Goggin, R.R.M. Paterson, Oil palm in the 2020s and beyond: challenges and solutions, CABI Agric. Biosci. 2 (1) (2021) 39, https://doi.org/10.1186/s43170-021-00058-3.

[10] O. Zaliha, C.L. Chong, C.S. Cheow, A.R. Norizzah, M.J. Kellens, Crystallization properties of palm oil by dry fractionation, Food Chem. 86 (2) (2004) 245–250, https://doi.org/10.1016/j.foodchem.2003.09.032.

[11] K. Sato, Polymorphic properties of palm oil and its major component triacyglycerols. Palm Oil., Elsevier, 2012, pp. 393–429, https://doi.org/10.1016/B978-0-9818936-9-3.50017-4.

[12] R.K.A. Garcia, K. Moreira Gandra, D. Barrera-Arellano, Development of a zero trans margarine from soybean-based interesterified fats formulated using artificial neural networks, Grasas Aceites 64 (5) (2013) 521–530, https://doi.org/10.3989/gya.049113.

[13] N.L Habi Mat Dian, Palm oil and Palm kernel oil: versatile ingredients for food applications, J. Oil Palm Res. 29 (4) (2018) 487–511, https://doi.org/10.21894/jopr.2017.00014.

[14] H. Górska-Warsewicz, K. Rejman, W. Laskowski, M. Czeczotko, Butter, margarine, vegetable oils, and olive oil in the average Polish diet, Nutrients 11 (12) (2019), https://doi.org/10.3390/nu11122943.

[15] K.K. Dash, M. Sharma, A. Tiwari, Heat and mass transfer modeling and quality changes during deep fat frying: a comprehensive review, J. Food Process Eng. 45 (4) (2022), https://doi.org/10.1111/jfpe.13999.

[16] W. Wongjaikham, G. Kongprawes, D. Wongsawaeng, K. Ngaosuwan, W. Kiatkittipong, P. Hosemann, S. Assabumrungrat, Production of low trans-fat margarine by partial hydrogenation of palm oil using nature-friendly and catalyst-free microwave plasma technique, Innov. Food Sci. Emerg. Technol. 80 (2022), https://doi.org/10.1016/j.ifset.2022.103107.

[17] M. Ziarno, D. Derewiaka, A. Florowska, I. Szymańska, Comparison of the spreadability of butter and butter substitutes, Appl. Sci. 13 (4) (2023), https://doi.org/10.3390/app13042600.

[18] G. Pande, C.C. Akoh, O.-M. Lai, Food uses of palm oil and its components, in: O-M Lai (Ed.), Palm Oil, 1st Ed., Elsevier, 2012, pp. 561–586, https://doi.org/10.1016/B978-0-9818936-9-3.50022-8.

[19] M.K. Gupta, Hydrogenation. in MK Gupta. Practical Guide to Vegetable Oil Processing, 2nd Ed., Elsevier, 2017, pp. 171–215, https://doi.org/10.1016/B978-1-63067-050-4.00007-6.

[20] T. Kim-Tiu, K. Nesaretnam, S. Kanagaratnam, Trans fats replacement solutions in Malaysia, in: D.R. Kodali (Ed.), Trans Fats Replacement Solutions, 1st Ed., Elsevier, 2014, pp. 385–398, https://doi.org/10.1016/B978-0-9830791-5-6.50023-X.

[21] E.D. Co, A.G. Marangoni, Organogels: an alternative edible oil-structuring method, J. Am. Oil Chem. Soc. 89 (5) (2012) 749–780, https://doi.org/10.1007/s11746-012-2049-3.

[22] M.D. Guillén, M.L. Ibargoitia, P. Sopelana, Margarine: composition and analysis. Encyclopedia of Food and Health, Elsevier, 2016, pp. 646–653, https://doi.org/10.1016/B978-0-12-384947-2.00446-3.

[23] A. Singh, F.-I. Auzanneau, M.A. Rogers, Advances in edible oleogel technologies – A decade in review, Food Res. Int. 97 (2017) 307–317, https://doi.org/10.1016/j.foodres.2017.04.022.

[24] A. Eilander, R.K. Harika, P.L. Zock, Intake and sources of dietary fatty acids in Europe: are current population intakes of fats aligned with dietary recommendations? Eur. J. Lipid Sci. Technol. 117 (2015) 1370–1377, https://doi.org/10.1002/ejlt.201400513.

[25] E.D. Heinle, J.C. Führ, N.S. Trindade, P. Fassina, J.P. Bruch-Bertani, F.S. Adami, Qualidade de vida, ingestão dietética e estado nutricional de idosos com mais de 80 anos institucionalizados, Res. *Soc. Dev.* 11 (17) (2022), https://doi.org/10.33448/rsd-v11i17.39096.

[26] E. Savelli, F. Murmura, The intention to consume healthy food among older Gen-Z: examining antecedents and mediators, Food Qual. Prefer. (2023) 105, https://doi.org/10.1016/j.foodqual.2022.104788.

[27] M. Kellens, V. Gibon, M. Hendrix, W. De Greyt, Palm oil fractionation, Eur. J. Lipid Sci. Technol. 109 (2007) 336–349, https://doi.org/10.1002/ejlt.200600309.

[28] P.K.P. Kumar, A.G.G. Krishna, Physico-chemical characteristics and nutraceutical distribution of crude palm oil and its fractions, Grasas Aceites 65 (2) (2014), https://doi.org/10.3989/gya.097413.

[29] M.K. Gupta, Winterization and fractionation of selected vegetable oils, in: M. K. Gupta (Ed.), Practical Guide to Vegetable Oil Processing, 2nd Ed., Elsevier, 2017, pp. 291–322, https://doi.org/10.1016/B978-1-63067-050-4.00011-8.

[30] S. Tong, T. Tang, Y. Lee, A review on the fundamentals of palm oil fractionation: processing conditions and seeding agents, Eur. J. Lipid Sci. Technol. 123 (2021), https://doi.org/10.1002/ejlt.202100132.

[31] P. Podchong, C.P. Tan, S. Sonwai, D. Rousseau, Composition and crystallization behavior of solvent-fractionated palm stearin, Int. J. Food Prop. 21 (1) (2018) 496–509, https://doi.org/10.1080/10942912.2018.1425701.

[32] Y. Wong, H. Hartina, Virgin coconut oil production by centrifugation method, Orient. J. Chem. 30 (2014) 237–245, https://doi.org/10.13005/ojc/300129.

[33] D.N. Taulbee, M. Mercedes Maroto-Valer, CENTRIFUGATION, in: *encyclopedia of Separation Science*, Elsevier (2000) 17–40, https://doi.org/10.1016/B0-12-226770-2/00011-9.

[34] S. Szepessy, P. Thorwid, Low energy consumption of high-speed centrifuges, Chem. Eng. Technol. 41 (2018) 2375–2384, https://doi.org/10.1002/ceat.201800292.

[35] *Separation High-Capacity Vacuum Filtration*, 1st ed. Andritz AG, Graz, Austria, 2021, Accessed: June 1st, 2025. [NN]. Available: https://www.andritz.com/resource/blob/13392/cf688eac900250897d0062f4b9df0407/se-yu-drum-filter-data.pdf.

[36] Filter Press Testing, Universal Filtration & Pumping Solutions, Inc., 2025. Accessed: June 1st, 2025. [Online]. Available: https://automaticfilterpress.com/filter-press-testing/.

[37] Filter Presses, 1st ed., McLanahan Co., Hollidaysburg, Pennsylvania, USA, 2025. June 1st, 2025. [Online]. Available: https://www.mclanahan.com/resource-library/filter-press-brochure.

[38] K.G. Clarke, Downstream processing. BioprocessEng, Elsevier, 2013, pp. 209–234, https://doi.org/10.1533/9781782421689.209.

[39] P.M. Doran, Unit Operations. Bioprocess Eng Principles, Elsevier, 2013, pp. 445–595, https://doi.org/10.1016/B978-0-12-220851-5.00011-3.

[40] T. Sparks, G. Chase, Solid–Liquid filtration – Examples of processes. Filters and Filtration Handbook, Elsevier, 2016, pp. 297–359, https://doi.org/10.1016/B978-0-08-099396-6.00005-8.

[41] D. Canizares, P. Angers, C. Ratti, A proposal standard methodology for the characterization of edible oil organogelation with waxes, Grasas Aceites 71 (2) (2020), https://doi.org/10.3989/gya.0106191.

[42] D. Canizares, P. Angers, C. Ratti, Organogelation capacity of epicuticular and cuticular waxes from flax and wheat straws, J. Am. Oil Chem. Soc. 98 (3) (2021) 329–339, https://doi.org/10.1002/aocs.12441.

[43] A.I. Blake, E.D. Co, A.G. Marangoni, Structure and physical properties of plant wax crystal networks and their relationship to oil binding capacity, J. Am. Oil Chem. Soc. 91 (6) (2014) 885–903, https://doi.org/10.1007/s11746-014-2435-0.

[44] F.R. Lupi, D. Gabriele, V. Greco, N. Baldino, L. Seta, B. Cindio, A rheological characterisation of an olive oil/fatty alcohols organogel, Food Res. Int. 51 (2) (2013) 510–517, https://doi.org/10.1016/j.foodres.2013.01.013.

[45] A. Mannan, K.R. Kazmi, M.S. Khan, I.H. Khan, A method for the determination of relative crystallinity of minerals by X-ray diffraction, Pak. J. Sci. Ind. Res. 49 (2) (2006) 72–76.

[46] S. Pollizi, G. Fagherazzi, A. Benedetti, M. Battagliarin, T. Asano, A fitting method for the determination of crystallinity by means of X-ray diffraction, J. Appl. Crystallogr. 23 (1990) 359–365, https://doi.org/10.1107/S0021889890004939.

[47] D.C. Montgomery, Design and Analysis of Experiments, 5th Edition, John Wiley & Sons, Inc, United States of America, 2001.

[48] R.W. Hartel, Crystallization in Foods, Aspen Publishers, Gaithersburg, Md, 2001.

[49] A. Selaković, I. Nikolić, L. Dokić, D. Šoronja-Simović, O. Šimurina, J. Zahorec, Z. Šereš, Enhancing rheological performance of laminated dough with whole wheat flour by vital gluten addition, LWT 138 (2021) 110604, https://doi.org/10.1016/j.lwt.2020.110604.

[50] B. Macias Rodriguez, A.G. Marangoni, The fat in a perfect croissant, Phys. Today 71 (1) (2018) 70–71, https://doi.org/10.1063/PT.3.3828.

[51] M. Öğütcü, E. Yılmaz, Oleogels of virgin olive oil with carnauba wax and monoglyceride as spreadable products, Grasas Aceites 65 (2014) e040, https://doi.org/10.3989/gya.0349141.

[52] M. Öğütcü, E. Yılmaz, Comparison of the pomegranate seed oil organogels of carnauba wax and monoglyceride, J. Appl. Polym. Sci. 132 (2015) app.41343, https://doi.org/10.1002/app.41343.

[53] M. Öğütcü, E. Yılmaz, Characterization of hazelnut oil oleogels prepared with sunflower and carnauba waxes, Int. J. Food Prop. 18 (2015) 1741–1755, https://doi.org/10.1080/10942912.2014.933352.

[54] R.B. Bird, W.E. Stewart, E.N. Lightfoot, Transport Phenomena, 2nd Edition, John Wiley & Sons, Inc, USA, 2002.

[55] T. Inoue, Strain-induced birefringence of amorphous polymers and molecular design of optical polymers, ACS Appl. Polym. Mater. 3 (5) (2021) 2264–2273, https://doi.org/10.1021/acsapm.1c001.